Robotica (2023), **41**, pp. 833–849
doi:10.1017/S0263574722000844

CAMBRIDGE UNIVERSITY PRESS

RESEARCH ARTICLE

Muscle weakness assessment tool for automated therapy selection in elbow rehabilitation

Sakshi Gupta, Anupam Agrawal and Ekta Singla*

Department of Mechanical Engineering, Indian Institute of Technology Ropar, Rupnagar, India
*Corresponding author. E-mail: ekta@iitrpr.ac.in

Received: 15 November 2021; **Revised:** 27 February 2022; **Accepted:** 15 May 2022; **First published online:** 23 June 2022

Keywords: rehabilitation robotics, task-based device, upper-limb exoskeleton, muscles weakness assessment tool, electromyography

Abstract

Clinical observations and subjective judgements have traditionally been used to evaluate patients with muscular and neurological disorders. As a result, identifying and analyzing functional improvements are difficult, especially in the absence of expertise. Quantitative assessment, which serves as the motivation for this study, is an essential prerequisite to forecast the task of the rehabilitation device in order to develop rehabilitation training. This work provides a quantitative assessment tool for muscle weakness in the human upper limbs for robotic-assisted rehabilitation. The goal is to map the assessment metrics to the recommended rehabilitation exercises. Measurable interaction forces and muscle correlation factors are the selected parameters to design a framework for muscular nerve cell condition detection and appropriate limb trajectory selection. In this work, a data collection setup is intended for extracting muscle intervention and assessment using MyoMeter, Goniometer and surface electromyography data for upper limbs. Force signals and human physiological response data are evaluated and categorized to infer the relevant progress. Based upon the most influencing muscles, curve fitting is performed. Trajectory-based data points are collected through a scaled geometric Open-Sim musculoskeletal model that fits the subject's anthropometric data. These data are found to be most suitable to prescribe relevant exercise and to design customized robotic assistance. Case studies demonstrate the approach's efficacy, including optimally synthesized automated configuration for the desired trajectory.

1. Introduction

Robotic treatment is becoming increasingly popular among patients suffering from neurological and musculoskeletal problems. Rehabilitation devices are used to help patients restore lost motor abilities. Manual or mechanical treatment is usually the only option for such patients to regain their motor abilities. Since there is repetition in specified exercises, manual assistance is difficult, time-consuming, and uncomfortable for the physiotherapist. Robotic rehabilitation is, therefore, a viable option [1, 2, 3]. It can deliver high doses of motor instruction at a reasonable cost. Nonetheless, training is dependent on one-on-one interaction between a therapist and a patient in the historical setting; as a result, rehabilitation is expensive and time-consuming. In addition, the dosage is usually insufficient for adequate recovery. Previous research has focused on building robotic rehabilitation systems for patients with muscular and neurological disorders, but their practical application in clinics and homes has been limited. Robotic training is considered less effective than dose-matched motor training, provided by therapists [4].

Task-oriented training is a research paradigm for upper extremity rehabilitation that includes three design concepts: skill development for functional activities, active participation training, and customized adaptive training. Recognizing a patient's weakness and assigning appropriate tasks is challenging [5, 6]. To understand a patient's functioning capability is essential to give appropriate therapy [7, 8]. Constructive muscular engagement suited to the patients' needs would help manage and adjust

their activities-of-daily-living. The most common techniques for measuring a patient's motor function are clinical scales and kinematic analysis. The Fugl–Meyer assessment, Oxford scale, Kendall scale, Ashworth scale, and a variety of other clinical measures are often used to assess upper limb functions [9, 10]. Since these clinical measurements are semi-quantitative techniques [8, 11], it is difficult to distinguish the significant influence on muscle function and motor coordination during the rehabilitation process. As a result, detecting substantial changes in the patient's motor movement using clinical measures is challenging. On the other side, due to the lack of quantifiable data on intervention effects and efficacy of various training protocols, the utility is limited across institutes and therapists [12, 13].

The surface electromyography (sEMG) and kinetic measures are essential tools in the study of movement because these can provide an electrophysiological perspective of motion. Researchers look at the effect of diminished dexterity on muscle activation post-injury [14]. The relationship between the post-stroke upper limb muscle weakness, co-contraction and clinical assessments of upper limb motor deficits and a physical handicap is examined by recording sEMG activity of paretic and non-paretic wrist flexors during isometric wrist flexion and extension [15]. Several studies have been conducted on mathematical and black box models to predict joint torque based on forces generated by muscle contraction. The Hill-based muscle model is a three-element model of mechanical muscle response used to convert sEMG signals to joint torque to maintain arm posture [16]. Callavaro et al. converted sEMG data using polynomial equations for joint torque prediction [17]. Using genetic algorithm (GA), researchers on sEMG have performed detection, analysis, feature extraction, and joint torque estimate [18]. Regression analysis is utilized to estimate joint torque based on the best-fit mathematical model [19]. According to several recent studies, the optimum way to deduce a mathematical model for predicting joint torque is exponential equations [20, 21].

The research goal of the current study is to develop a quantitative statistical technique for weakness estimation and is capable of deciding the recommended exercise. When a person is connected to a robotic system, muscle weakness evaluation is essential to forecast the task for the rehabilitation device to create rehabilitation training. Figure 1 briefly explains the technique used in the present work for biomechanical–based joint motion reconstruction. The study used sEMG signals and force sensors to assess impairment and muscle engagement during elbow flexion/extension movement. A comparative analysis is used to identify the dominant muscle during elbow flexion motion, with the results confirmed using the Open-Sim software. Using a mathematical model, the force interaction is connected to the sEMG signals corresponding to the dominant upper arm muscle. The Pearson product correlation moment is computed to verify the efficient and successful rehabilitation training attempts. Anthropometric subject data are used to extract the necessary trajectory data points. Two realistic case studies are included to demonstrate the proposed algorithm framework as a tool for mapping weakness to robotic task planning.

2. Experimental setup and methodology

This section details the method for predicting a patient's weakness to identify the task for the rehabilitation device in establishing rehabilitation training. The subjects' elbow moment signals, sEMG signals, contact force signals, and natural human motion data are gathered for the study. Butterworth Low-Pass filter and crucial damping low-pass filtering are used to pre-process sensors data. This section has five stages: experiment setup and data acquisition, identification of dominant muscles by signal processing, correlation analysis, quantitative model estimation, and rehabilitation task planning.

2.1. Experimental setup and dataset acquisition

An experimental setup for elbow flexion/extension movement has been developed. The experimental setup consists of a MyoMeter sensor (M-550), wireless Goniometer (W-series) sensor, and LE-230 DataLite wireless sEMG sensors. These sensors have been purchased from the United Kingdom-based firm Biometrics Ltd to test muscle intervention and assessment. During the process, individuals are

https://doi.org/10.1017/S0263574722000844 Published online by Cambridge University Press

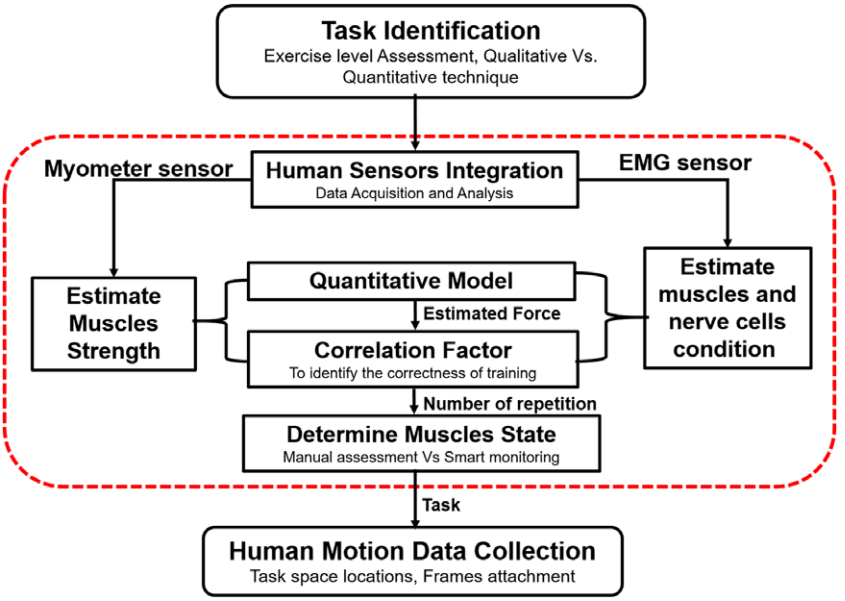

Figure 1. *Mapping of task planning to task-based robotic synthesis through automatic muscle weakness assessment tool.*

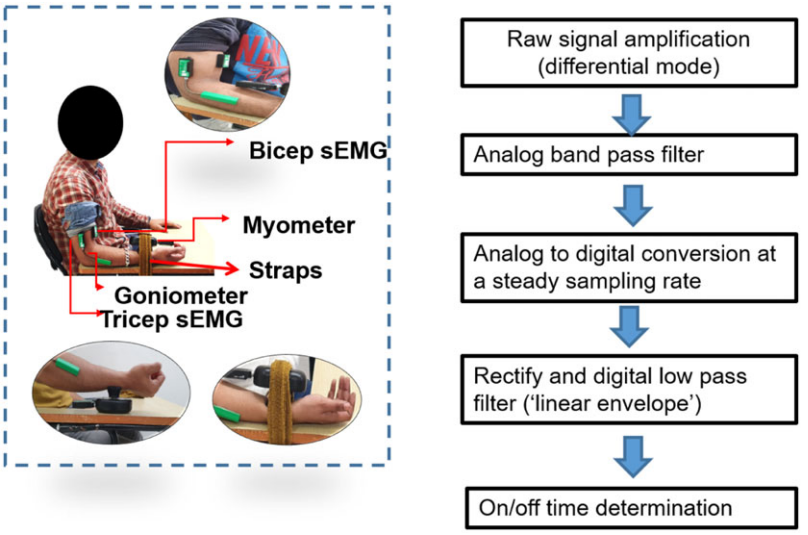

Figure 2. *Data acquisition and signal processing.*

instructed to utilize their right hand; an extra harness system is primarily employed to keep the subject's hand secure and to limit wrist mobility to a substantial degree. The body positions are demonstrated in Fig. 2(a), with the upper arms flexed to 0° and forearms flexed to 90°. The sensors' reaction is explicitly tested for the biceps brachii and triceps brachii muscles during elbow flexion movement. The expected contact force is measured in real time using a wireless wrist-mounted Myometry sensor. Muscle activity is monitored using wireless sEMG sensors placed on the two aforementioned muscles during the elbow flexion. Wireless Goniometer sensors are used to track movement during exercise.

https://doi.org/10.1017/S0263574722000844 Published online by Cambridge University Press

Table I. *Details of subjects demographic and health information. Here, SD represents standard deviation.*

Characteristics			**Values**
Gender		Female	02
		Male	08
Age (in years)		Mean ± SD	42.5 ± 17.5
		Range	25–60
Height (m/feet)		Mean ± SD	1,73 ± 0.04
Weight (kg)		Mean ± SD	67.5 ± 8
Dominant arm			Right
	Upper arm (m)	Mean ± SD	0.31 ± 0.03
Right arm	Lower arm (m)	Mean ± SD	0.27 ± 0.02

The data set contains motion data from 10 healthy subjects, 8 men and 2 women, ranging in age from 25 to 60 years old and weighing 50 to 75.5 kg, with their consent. The subject name protocol provides letters to distinguish male and female participants, as well as the subject's serial number. For example, F_{001} denotes a female candidate with a serial number of one. Table I displays the demographics and health information of the individuals.

2.2. Dominant muscle identification using signal processing framework

The task is performed on the participants' dominant arms. The angular displacements of the elbow joint are measured using a wireless Goniometer sensor. Sensors' data are captured as analog signals, then smoothed and rectified using a digital low-pass filter. The sEMG signals from biceps brachii and triceps brachii are acquired from two selected muscles. Figure 2(b) depicts the analysis of the sEMG signals. The signal is recorded in differential mode, measuring the voltage difference between two electrodes. Before being digitized, the raw signal is subjected to analog filtering, most often band pass. Low and high frequencies are removed from the signal via band-pass filtering. The low-frequency cut-off is taken between 5 and 20 Hz, and the high frequency is taken as 200 Hz – 1 kHz [22]. The sampling rate is adjusted to at least twice the analog low-pass filter's cut-off frequency. A digital high-pass filter to the stream is applied to eliminate movement and other artifacts. The 6th order, 20 Hz high-pass filter, is employed to rectify and digitize the low-pass filter in the next step, where the signal's absolute value is taken. The instances are identified to estimate on and off periods when the signal's envelope (derived by removing mean value, rectifying, and applying a digital low-pass filter to the signal) exceeds a threshold. The threshold can be established by several factors, including:

$$Threshold = \mu + 3 * \sigma, \tag{1}$$

where, μ and σ denote mean and standard deviation, respectively.

Algorithm 1 illustrates the procedure for extracting a linear envelope of signals. Figures 3 and 4 shows the raw data and processed data to extract linear envelope for a sample of biceps brachii and triceps brachii sEMG signals, respectively. Consequently, the sensors data have been analyzed for depicting all individuals' sEMG sensors data for the biceps brachii and triceps brachii and for identifying substantial influences on upper arm movement.

2.3. Correlation analysis

Understanding the relationship between the muscles and the applied force is essential for task and interaction force control. To assess the relationship between the contact forces and the muscle responses, the Pearson product–moment correlation criteria (see Eq. (2)) are utilized. The correlation factor between

https://doi.org/10.1017/S0263574722000844 Published online by Cambridge University Press

Algorithm 1 Computation of linear envelope for a signal

1: Initialize low pass filter frequency (F).
2: Initialize sampling rate n.
3: Load sEMG raw data x.
4: Compute Nyquist frequency ($n/2$).
5: Estimate full wave rectification (abs(x - *mean*(x))).
6: Specifies the intended frequency of the final cutoff 20 Hz.
7: Apply 2nd order Butterworth low pass filter (25% adjustment factor).
8: Determine signals' envelope.
9: Determine threshold value $= \mu + 3 * \sigma$.
10: Plot the data vs time: raw data in blue, rectified data in green, and linear envelope in red.

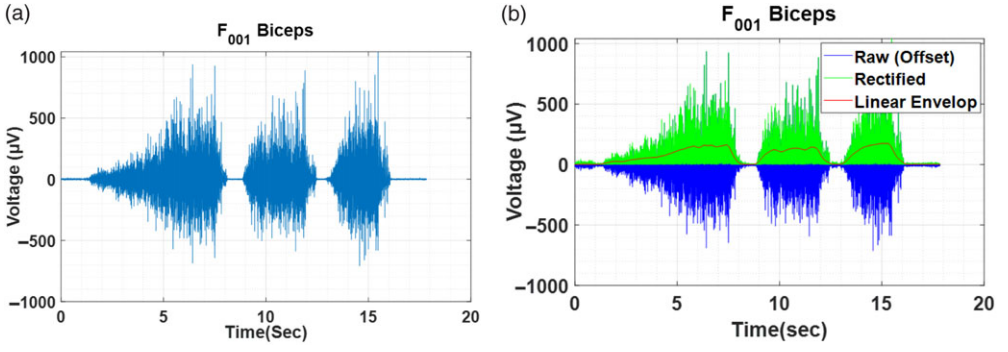

Figure 3. *A sample subject's biceps brachii muscle responses while undergoing elbow flexion/extension exercise with three trials: (a) Pictorial representation of raw sEMG responses and (b) Processed sEMG responses to extract linear envelope.*

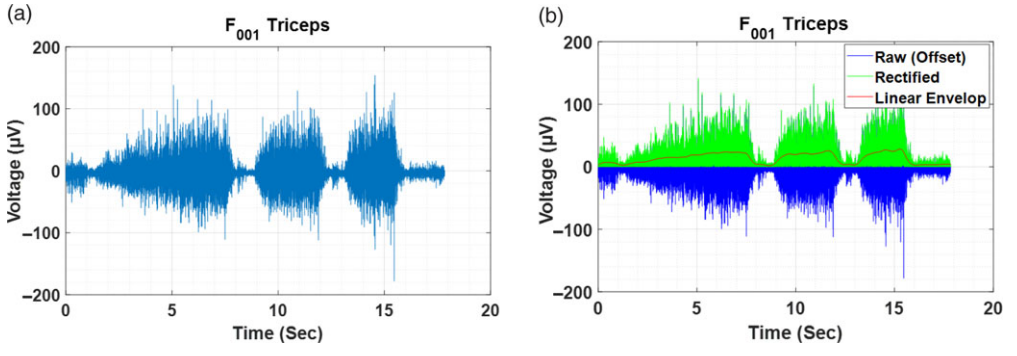

Figure 4. *A sample subject's triceps brachii muscle responses while undergoing elbow flexion/extension exercise with three trials: (a) Pictorial representation of raw sEMG responses and (b) Processed sEMG responses to extract linear envelope.*

the sensor data is used to reveal the redundant inputs and outputs and feature reduction and selection procedures—given the fact that the more linked the system is, the higher the correlation factor.

$$r = \frac{\sum (x_i - \bar{x})((y_i - \bar{y})}{\sqrt{(x_i - \bar{x})^2((y_i - \bar{y})^2}} \tag{2}$$

https://doi.org/10.1017/S0263574722000844 Published online by Cambridge University Press

Here, r = correlation coefficient, x_i= value of muscle responses, $\bar{x}$ = mean of the value of the muscle response, y_i = value of contact forces, and $\bar{y}$ = mean of the value of the contact forces.

2.4. Quantitative model and estimation

A mathematical model is required to convert sEMG signals of dominant muscle into muscle force estimation. The study utilizes the curve-fitting approach to identify the best fit mathematical model. An optimization problem is formulated using the Levenberg–Marquardt technique to minimize the error between the estimated and the actual forces (represented in Eq. (3)).

The fitness value is calculated by averaging the error percentages from all the data points.

$$Error = \sum_{i=1}^{n} \frac{(f_{est})_i - (f_{act})_i}{N_i}. \tag{3}$$

Here, f_{est} denotes estimated force and f_{act} denotes actual force. N denotes data set size, and n denotes sample rate. The coefficients A_0, A_1, B_1, and W play a crucial role in determining the simulated muscles strength based on sEMG signals.

The sum-of-squared errors (SSE), root mean square error (RMSE), and coefficient of determination (R-square) are the parameters used to evaluate the most appropriate model. SSE is calculated as the sum of the squared differences between the observed value and the predicted value, and a smaller value is preferable. The RMSE is defined as the standard deviation of the residuals (prediction errors) and must be less than one. The R-square is defined as the proportion of variation predicted by the independent variable in the dependent variable, and its value ranges from 0.1 to 1. A model with a greater value is preferred.

2.5. Rehabilitation task planning

This section maps the collected muscle activity information to the rehabilitation task planning by integrating recommended exercises. This provides the tasks to the customized robotic system designers.

2.5.1. Task identification

Task-oriented rehabilitation retrains human movements by providing standard physical tools in different spatial locations, allowing users to execute assigned activities. Moreover, the joint range-of-motion (ROM) and muscular flexibility must be sufficient to enable correct functional excursions of the muscles and bio-mechanical alignment [23, 24]. The research exclusively collects natural human motion data utilizing joint flexibility exercises (i.e. ROM exercises) to strengthen weak muscles. To establish the concept, the workouts assumes to be planar, and the focus is on elbows flexion/extension joint motion range. Figure 5(a) shows elbow flexion/extension joint motion range (sagittal plane) when the shoulder flexion angle is fixed at 0°. A similar procedure can be implemented to other recommended exercises.

2.5.2. Trajectory generations

To indicate the location and orientation of a robotic link about adjacent links, the Denavit–Hartenberg (D–H) convention is utilized. It is crucial to select a specific motion trajectory to plan a robot's mobility by providing initial values for joint variables. The experimental setup, depicted in Fig. 5(b), is intended to collect natural human motion data to follow the therapeutically required motion trajectory. Here, task space locations (TSLs) are a set of coordinates that indicate the wrist positions of the participants. Trajectories are traced out to get realistic human motion trajectories corresponding to recommended rehabilitation exercises.

https://doi.org/10.1017/S0263574722000844 Published online by Cambridge University Press

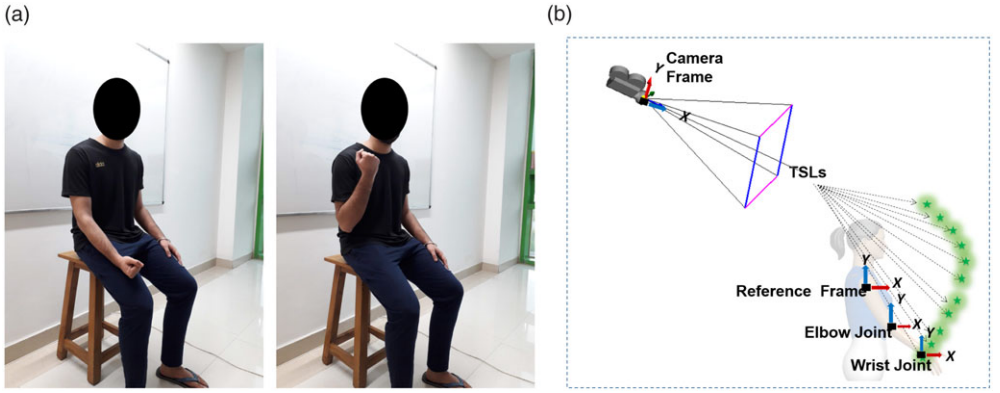

Figure 5. *(a) Joint ROM exercise for muscular flexibility performing elbow flexion/extension when shoulder flexion angle is at* 0° *(parallel to sagittal plane), Courtesy: Indian Spinal Injury Centre, New Delhi, India. (b) Experimental setup for human motion data collection.*

Algorithm 2 Scaling musculoskeletal model

1: Initialize D-H parameters for static pose (link length, joint offset, twist angle, joint angle)
2: Define D-H parameter in Robo-Analyzer software
3: Set time duration and number of steps (t,n)
4: Compute forward kinematics
5: Extract data points for static pose
6: Import in Open-Sim as a markers data for static pose
7: Compute scale factor using Open-Sim GUI
8: Run the simulation

Both marker-based and marker-less data collection techniques for human mobility have been used in the past. The investigation has included simulations of dynamic movement, and neuromuscular coordination and physical performance have been examined. Additionally, simulators provide a scientific basis for therapy planning by identifying the source of abnormal activity. Towards this, the study has collected previously revealed participants' natural human motion data sets, created utilizing scaled Open-Sim upper extremity musculoskeletal models. It aims that Open-Sim could simulate movement quickly and accurately. To begin with, the programme anticipates natural motion coordinate data by using motor control models, such as kinematic adaptations of human gestures at various phases. A tool named Robo-Analyzer is used to accelerate the kinematic model framework. It may also inspect each D–H parameter by selecting an individual joint and then the kind of D–H parameter. The appropriate D–H parameter is highlighted in the D–H parameters input table when a transformation frame is applied to the robot model.

Algorithm 2 shows the step-by-step procedure to obtain the subject-specific scaled musculoskeletal model. A large data set of joint coordinate trajectories is obtained using the simulations. The article does not provide a detailed analysis of the design of a trajectory-based rehabilitation device.

3. Results and discussion

Muscle involvement has been widely studied to identify substantial influences on upper arm movement. Consequently, the sensor's data have been analyzed. Figure 6 depicts all individuals' sEMG sensors data for the biceps brachii and triceps brachii. As expected, the considered activity is best suited for biceps brachii, whereas triceps brachii necessitates a different action. As a result, the biceps brachii,

https://doi.org/10.1017/S0263574722000844 Published online by Cambridge University Press

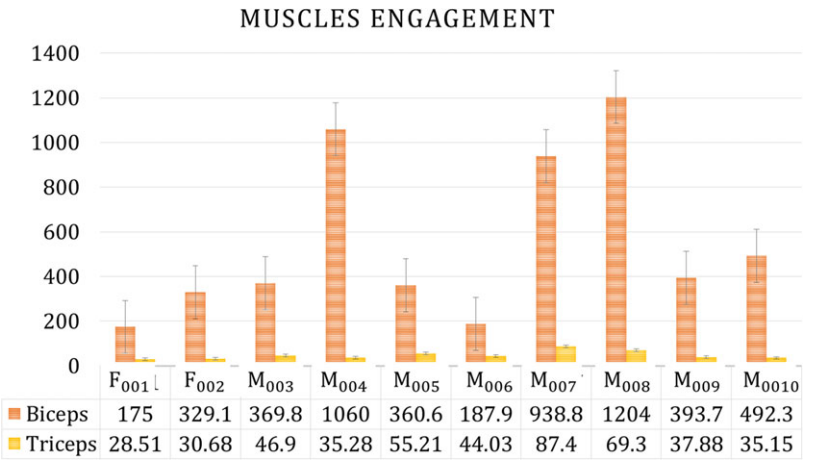

	F_{001}	F_{002}	M_{003}	M_{004}	M_{005}	M_{006}	M_{007}	M_{008}	M_{009}	M_{0010}
Biceps	175	329.1	369.8	1060	360.6	187.9	938.8	1204	393.7	492.3
Triceps	28.51	30.68	46.9	35.28	55.21	44.03	87.4	69.3	37.88	35.15

Figure 6. *A chart presenting a graphical depiction of the processed sEMG signal responses of the biceps brachii and triceps brachii muscles during elbow flexion/extension exercise for all ten participants.*

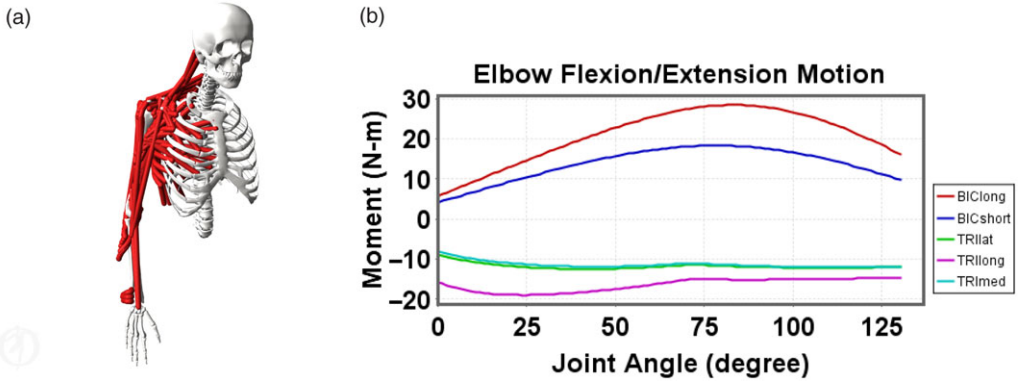

Figure 7. *Open-Sim software validating results for dominant muscle identification by simulating musculoskeletal model: (a) posture of upper extremity musculoskeletal model and (b) muscles involvement during task completion.*

regardless of human anatomy, has a considerably more significant influence on the outcome of the chosen activity.

Open-Sim simulation software is utilized to verify the outcomes of the study, as shown in Fig. 7. Open-Sim musculoskeletal models support the findings. When the same exercise is conducted using Open-Sim software, the biceps brachii sEMG signals exert a more substantial influence than the other muscles. This reduces dimensionality by eliminating parameters with high dominance. Based upon this, dominant muscle analysis identifies critical, independent aspects that aid in developing a mathematical model with fewer parameters.

The correlation of sEMG signals collected from the biceps brachii and triceps brachii muscle groups is investigated to determine the importance of interdependent muscle responses. The only correlation between sEMG signals obtained from biceps brachii and contact force received from the MyoMeter sensor is more significant than 0.9 (highlighted with a red square), which is significantly greater than the others. In contrast, the pattern and diversity of contact force and muscle activation correlations appear to be subjective for different persons, and averaged values are used. Figure 8 depicts the overall data. In almost all instances, the correlation between biceps brachii and interaction forces is significant

https://doi.org/10.1017/S0263574722000844 Published online by Cambridge University Press

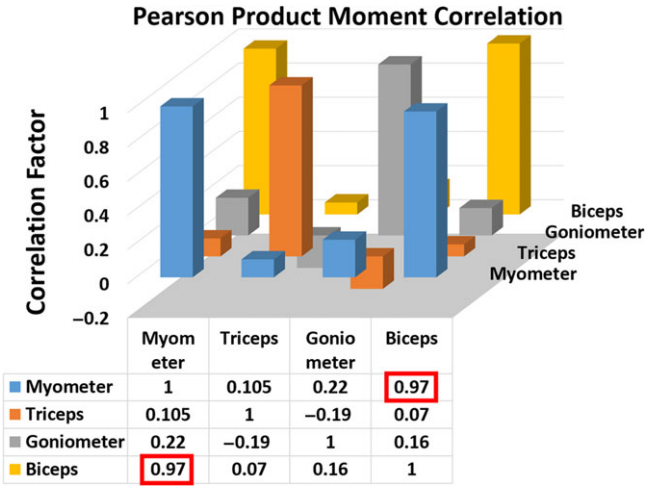

	Myometer	Triceps	Goniometer	Biceps
Myometer	1	0.105	0.22	0.97
Triceps	0.105	1	–0.19	0.07
Goniometer	0.22	–0.19	1	0.16
Biceps	0.97	0.07	0.16	1

Figure 8. *Correlation factor for combined data (all 10 participants).*

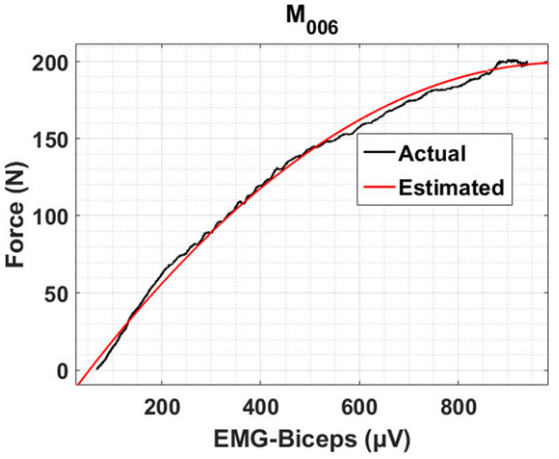

Figure 9. *Curve fitting of the estimated force to the actual force in graphical form (one of the participant).*

enough, which is preferable based on previous dominant muscle outcomes throughout the activity. This calculation can analyze a more robust and practical training and related rehabilitation progress.

Following that, as described in Section 2.4, standard Fourier series[1] is obtained as a suitable mathematical model for determining the quantitative and statistical value of the biceps brachii's muscular force. Figure 9 shows an example of a curve fitting match to the anticipated force to the actual force for an individual participant.

The comparative findings of the proposed model and Kim et al. [21] model for all 10 participants while executing the prescribed work, that is the elbow flexion motion, are displayed in Table II. The SSE, RMSE, and R-square for the proposed model have all been shown to be acceptable. Figure 10(a) represents comparison of the proposed model to actual data, and Kim et al. [21] model for one of the participant. The graph of the simulated model is found to be pretty close to the actual data. Additionally, the data from the Open-Sim musculoskeletal model are utilized to validate the proposed model, as seen

[1]The mathematical expression for Fourier series is $f_{est} = A_0 + A_1 * cos(X * W) + B_1 * sin(X * W)$, Where, f_{est} stands for muscular estimated force (in N), X signifies sEMG signals (in μV) and A_0, A_1, B_1, and W are the muscle coefficients.

https://doi.org/10.1017/S0263574722000844 Published online by Cambridge University Press

Table II. *Comparative results of proposed model and kim et al. [21] model for all 10 healthy participants in completing the assigned task, that is elbow flexion movement.*

	Proposed model			Kim et al. model [21]		
Subject	**SSE (n)**	**R-square**	**RMSE (N)**	**SSE (N)**	**R-square**	**RMSE (N)**
M_{003}	228.1	0.97	0.87	228.0	0.97	0.87
M_{004}	337	0.99	0.28	329.6	0.99	0.27
M_{005}	328.3	0.99	0.35	579.8	0.99	0.46
M_{006}	328.3	0.99	0.35	579.8	0.99	0.46
M_{007}	3710	0.98	0.77	–	–	–
M_{008}	219.7	0.99	0.38	–	–	–
M_{009}	117.4	0.98	0.73	–	–	–
M_{010}	252.2	0.99	0.21	–	–	–
F_{001}	109.6	0.98	0.28	749.9	0.98	0.23
F_{002}	175.3	0.98	0.22	–	–	–

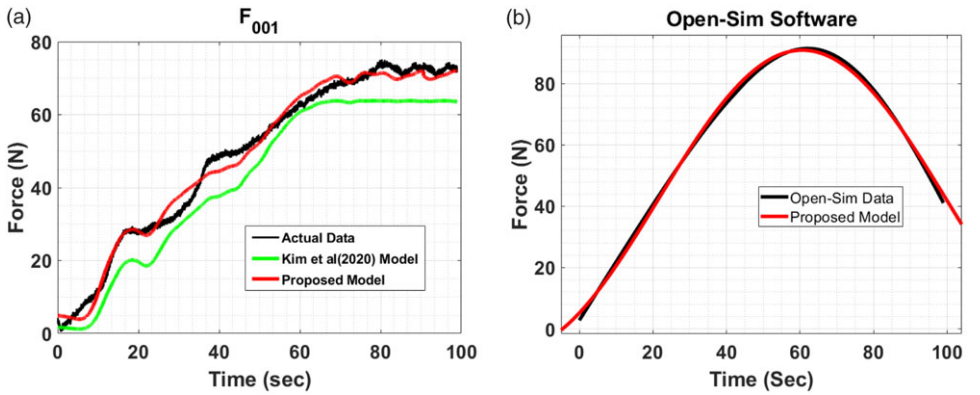

Figure 10. *(a) Comparison of an individual participant's actual data to Kim et al.'s model and proposed model data, (b) Comparison of proposed model to Open-Sim musculoskeletal model data.*

in Fig. 10(b) where SSE 7.89 N, R-square 0.99, and RMSE 0.28 N are obtained. Hence, the proposed mathematical model based on the most influential muscle is demonstrated to be the best to predict the afflicted limb's quantitative weakening value (force).

Through trajectory generation, a large data set of therapeutically desired natural human motion trajectory is gathered, and for the sake of simplicity, just a few numbers are displayed in Table III for one of the participant. Here, the modified joint coordinates are shown to be following the shoulder joint as the reference frame.

3.1. Case Study 1: patient of quadriplegia (less than 3 months): demonstration

Medical and rehabilitation robots use human motion data to create various innovative recreational assistance devices that mimic the human body's natural motion. When it comes to identifying muscular weakness-based task locations of therapeutically needed trajectory for each patient, the recommended technique will play a satisfying role. This case involves a 30-year-old man who has quadriplegia. Both of his upper limbs have shown limited elbow flexion movement during movement. The proposed algorithm's framework is used to choose an experimental setting for evaluating weak muscle and tracking its recovery in a way that mimics the joint biological trajectory. Data have been collected from Spinal Injury

https://doi.org/10.1017/S0263574722000844 Published online by Cambridge University Press

Table III. *Using Open-Sim software, transformed human motion data of the wrist with respect to the shoulder as a reference frame (one of the participants).*

TSLs	X_{wrist}(m)	Y_{wrist}(m)
P_1	0	−0.52
P_2	0.05	−0.51
P_3	0.12	−0.48
P_4	0.18	−0.44
P_5	0.22	−0.39
P_6	0.25	−0.28
P_7	0.22	−0.15

Figure 11. *Case Study 1: Some clicks of sensors integration with Patient of Quadriplegia (injury less than 3 months), Courtesy: Indian Spinal Injury Center (ISIC).*

Center, where the subject is a regular patient of Out-Patient Department (OPD). Disability is identified by sensors integration and data assessment. Figure 11 depicts the experimental setup, which consists of sensors integrated with human limb and can able to recognize muscle intervention and engagement, allowing for the mapping of weakness evaluation to task planning. Processed sensor data are utilized to determine Pearson product–moment correlation, and observed biceps brachii muscles have a higher correlation factor of 0.82 for weaker limb and 0.88 for weak limb. The Pearson product–moment correlation for the weaker limb is depicted in Fig. 12, with the higher correlation component highlighted in red.

The mathematical model is obtained with the measures SSE 328 N, R-square 0.95, and RMSE 0.28 N for weak limb and SSE 1572 N, R-square 0.77 and RMSE 6.46 N for weaker limb. As demonstrated in Fig. 13, the model has estimated the quantitative weakening value of the affected limbs as nearly 40 N for weaker limb and 70 N for weak limb. Motion data is collected via an Open-Sim scaled musculoskeletal

https://doi.org/10.1017/S0263574722000844 Published online by Cambridge University Press

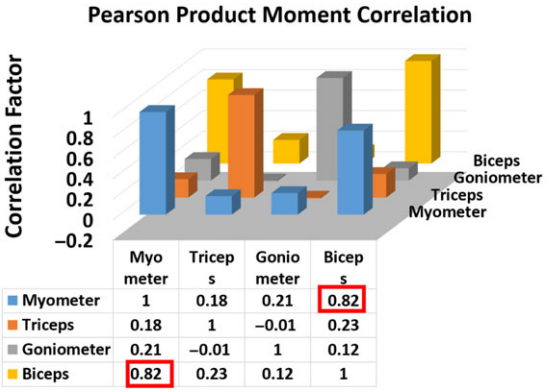

Figure 12. *Case Study 1: Illustration of Pearson Product Moment Correlation for the weaker limb.*

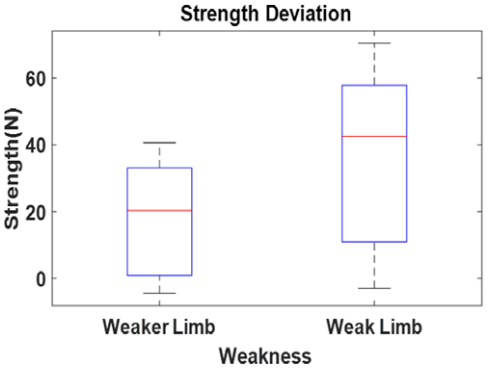

Figure 13. *Case Study 1: Comparison of disability between both upper extremity.*

model, which corresponds to anthropometric subject data and is obtained as displayed in Table IV. The corresponding clinically desired trajectory is shown in Fig. 14.

3.2. Case Study 2: patient of hemiplegia (less than 3 month): trajectory-based robotic assistance

This case study briefs the methodology for utilizing the proposed framework in robot-assisted rehabilitation. Figure 15 showcases the connectivity chart where the weakness information is extracted in the first step by sensors integration with the human limb. The proposed quantitative measures, namely muscle intervention and muscle engagement, are used in the previous case. In the second step, the task is planned according to these outcomes of muscles intervention and the automatically recommended therapy. This task information, such as task type and task space locations', is depicted in the third phase of Fig. 15. It is used to build a model that optimizes the dimensional parameters of a data-driven mechanism. The evolutionary algorithm is utilized to optimize the synthesis problem. The final step in Fig. 15 exposes the designer's sorting criteria, such as kinematic performance index and reachability, to choose the best performing mechanism. The example concludes by demonstrating how the proposed algorithmic technique would give a general framework for task-based robotic-assisted dimensional synthesis from automated therapy selection and data collection.

This case involves a 50-year-old female patient with hemiplegia. The patient has limited elbow flexibility in her right upper limb. Correlation coefficients are calculated to measure the present relationship strength between sensor data, indicating the action's dependability for the targeted muscles. As demonstrated in Fig. 16, the significant relationship between the biceps brachii sEMG signals and

https://doi.org/10.1017/S0263574722000844 Published online by Cambridge University Press

Table IV. *Case Study 1: Collecting natural human motion data using a scaled Open-Sim musculoskeletal model that corresponds to the participant's anthropometric data for the weaker limb.*

TSLs	X_{wrist}(m)	Y_{wrist}(m)
P_1	0	−0.70
P_2	0.06	−0.70
P_3	0.14	−0.67
P_4	0.27	−0.56
P_5	0.33	−0.44
P_6	0.33	−0.32
P_7	0.29	−0.20

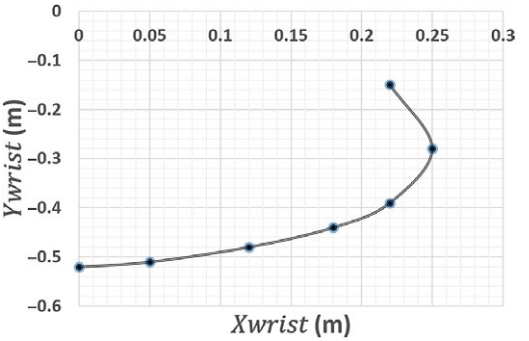

Figure 14. *Case Study 1: Graphical depiction of the therapeutically desirable natural human motion trajectory.*

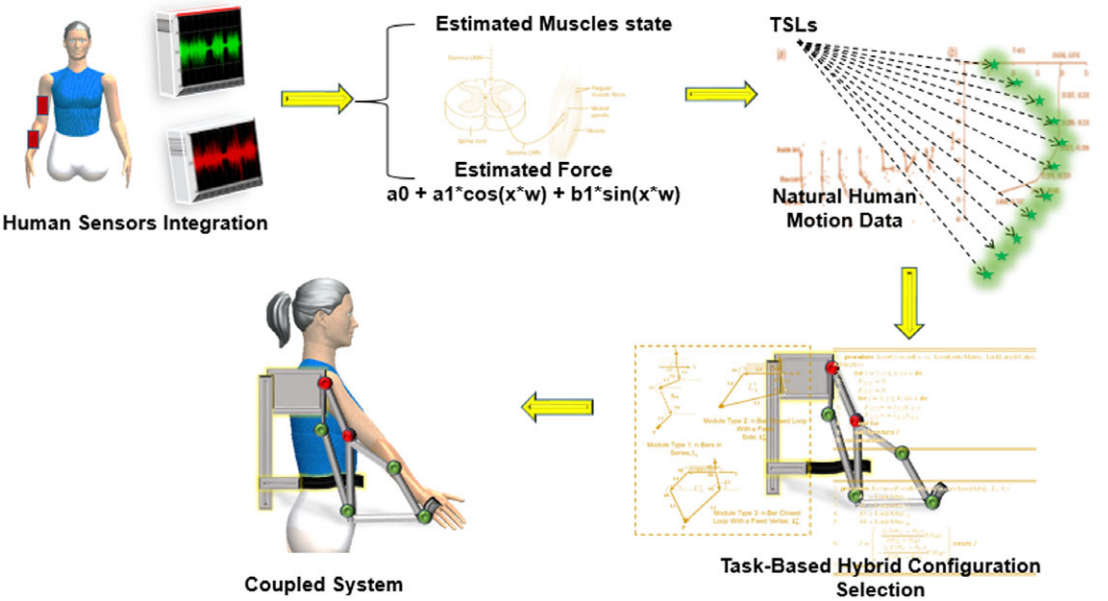

Figure 15. *Steps being taken in the development of trajectory-oriented robotic assistance systems.*

https://doi.org/10.1017/S0263574722000844 Published online by Cambridge University Press

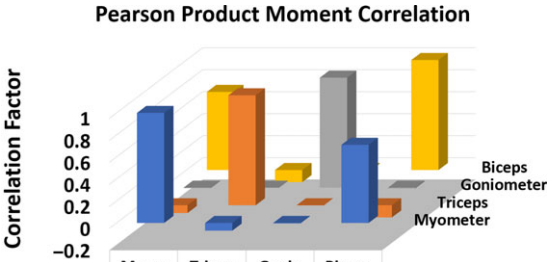

	Myometer	Triceps	Goniometer	Biceps
Myometer	1	−0.07	−0.004	0.71
Triceps	−0.07	1	−0.001	−0.11
Goniometer	−0.004	−0.001	1	−0.007
Biceps	0.71	−0.11	−0.007	1

Figure 16. *Case Study 2: Illustration of Pearson Product Moment Correlation for the effected limb.*

the MyoMeter is less than 0.9 and higher than others. A better correlation between Biceps Brachhii and MyoMeter sensor indicates the accuracy of training attempts directed at the targeted muscle. The developed model provides a SSE 87.68 N, R-square 0.99, and RMSE 0.16 N. The model has estimated the quantitative weakness value of the affected limb is less than 5 N. Consequently, it is suggested to repeat the exercise to acquire the quantitative connection between biceps brachii motor functions similar to healthy ones. Therefore, the quantitative model for force prediction would aid healthcare in comparative analysis. Subject anthropometric data are utilized to create an Open-Sim scaled musculoskeletal model. The results of the data analysis of muscle weakness assessment to task planning, which turned the co-ordinate measurements of the shoulder and wrist position, with the shoulder as the local co-ordinate frame (reference frame). TSLs show the trajectory data points generated from the Open-Sim scaled musculoskeletal model. Table V represents the upper limb recommended trajectory.

Case study 2 is expanded further to showcase the remaining two phases. This is achieved by determining the optimal dimensions for a four bar with a single bar configuration. The objective of the synthesis problem is to achieve a trajectory while optimizing kinematic performance and maintaining a high level of positional accuracy. The selection of configuration is not part of the paper. Jacobean conditioning index and reachability are being used to evaluate the best. The former ensures the mechanism's kinematic performance at given places, while the latter provides the correctness of the end-positional point at defined trajectory points. The anthropometric data from the human upper-limb is being used to calculate link length variations and joint-angle ranges of the selected configuration. The multi-model problem is tackled using the GA, an evolutionary technique. For each candidate, link lengths (L) and joint angles (θ) are utilized to derive the objective functions and constraints of the specified issue (solution).

The obtained optimal link lengths for the four bar with a single-bar mechanism have been determined using dimensional synthesis as $L_1 = 0.07$ m, $L_2 = 0.23$ m, $L_3 = 0.006$ m, $L_4 = 0.27$ m, and $L_5 = 0.29$ m. The base link has an angle of $\theta_3 = 180°$. The reachability error is determined to be 0.001 m, which falls within the tolerance level. As demonstrated in Fig. 17, the results for reachability at each TSL are provided for this four-bar structure connected with single bar. The conditioning index varies from 0.1 to 0.84 for the specified collection of TSLs. The best postures are observed from P_3 onwards. The contours are plotted for active angles θ_1 from 0° to 360° and θ_5 from 0° to 360°, respectively, as shown in Fig. 18(a). Corresponding manipulability plot is shown in Fig. 18(b) and workspace region is shown in Fig. 18(c). Table VI shows optimal synthesis findings for the configuration at all TSLs data points, together with active joint angles, conditioning index, and manipulability.

Anthropometric subject data is being utilized to determine the amount of assistive torque required as the link weight is assumed to be negligible [25]. As a percentage of total body weight, upper arm segment weight is 2.9% for women and 3.25% for men, while the lower arm segment weight is 1.57% for women and 1.87% for males [26]. The healthy limb's gravitational factor is determined to be 25.11 N to move the

https://doi.org/10.1017/S0263574722000844 Published online by Cambridge University Press

Table V. *Case Study 2: Natural human motion data collection utilizing a scaled model of Open-Sim software that corresponded to the anthropometric data of the participant.*

TSLs	X_{wrist}(m)	Y_{wrist}(m)
P_1	0	−0.56
P_2	0.09	−0.54
P_3	0.19	−0.48
P_4	0.23	−0.43
P_5	0.25	−0.38
P_6	0.26	−0.31
P_7	0.26	−0.23

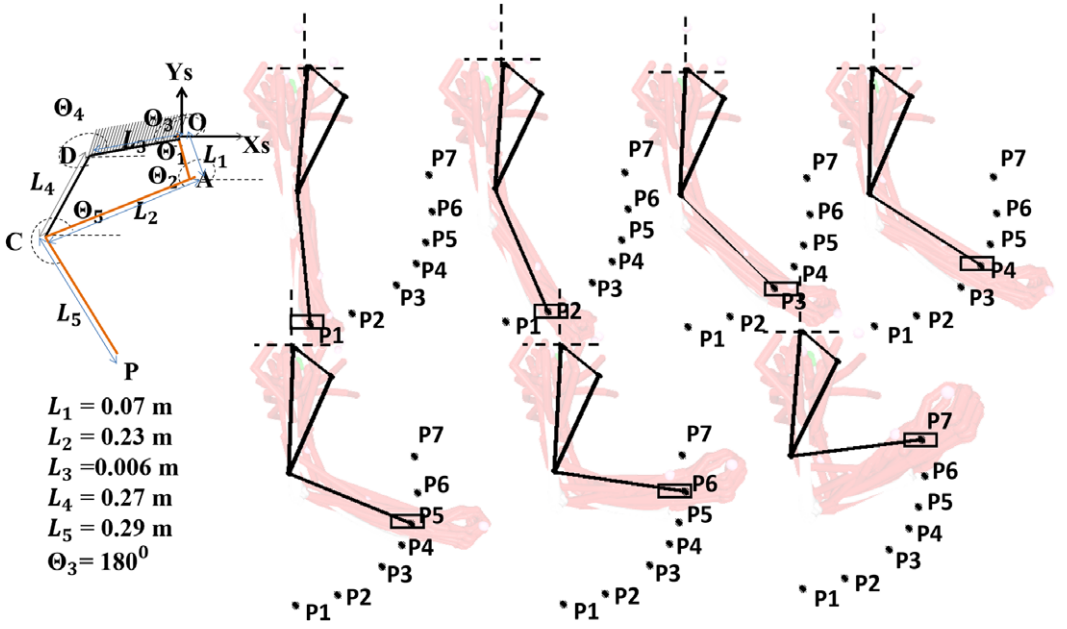

Figure 17. *Case Study 2: Optimal synthesized results based upon clinical trajectory.*

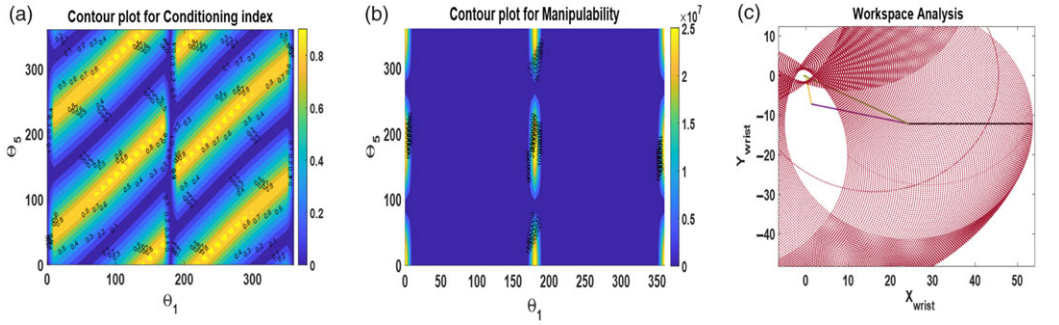

Figure 18. *Case Study 2: Results of workspace computation and singularity analysis for selected four bar with single-bar configuration: (a) Contours for conditioning index, (b) Contours for manipulability, and (c) Workspace analysis.*

https://doi.org/10.1017/S0263574722000844 Published online by Cambridge University Press

Table VI. *Case Study 2: Optimal synthesised results for the configurations for their corresponding active joint angles and conditioning index and manipulability at each TSLs data points.*

TSLs	θ_1	θ_5	1/c	M
P_1	310.59	276.82	0.10	146.76
P_2	313.48	293.38	0.24	341.11
P_3	314.82	315.39	0.44	552.58
P_4	316.05	327.53	0.55	636.99
P_5	315.36	337.37	0.67	698.22
P_6	314.27	351.58	0.84	741.00
P_7	312.64	7.23	0.77	729.13

Table VII. *Case Study 2: Torque requirement for elbow flexion/extension.*

TSLs	P1	P2	P3	P4	P5	P6	P7
$\tau_{actuator1}$(Nm)	−4.56	−4.75	−4.84	−4.94	−4.89	−4.80	−4.66
$\tau_{actuator2}$(Nm)	−6.52	−7.71	−8.29	−8.095	−7.65	−6.66	−5.08

forearm in the sagittal plane, and the torque for the healthy upper limb during elbow flexion/extension is estimated to be 3.5 Nm. In contrast, the torque for the afflicted (weak) limb is 0.68 Nm. The exoskeleton would be designed to provide 2.82 Nm of robotic assistance as a solution. Table VII takes into account the rated torque values required for both active actuators of the mechanism, which are determined to be between 4.56 and 4.94 Nm for actuator-1, that is almost constant, and 5.08 to 8.29 Nm for actuator-2. Here, a negative toque indicates clockwise rotation.

4. Conclusions

This paper proposed a methodology for quantifying the relationship between the metric for assessing muscle weakness and the therapeutically recommended exercise that serves as the task for the rehabilitation device. Measurable contact force and muscle correlation factors are chosen parameters for establishing a framework for detecting muscular nerve cell state and recommended appropriate limb trajectories. The study investigates a strong connection between biceps brachii sEMG signals and MyoMeter in healthy patients. The inter-correlation between biceps brachii and contact force is high enough to reduce them to a single representative variable. The Fourier curve-fitting method is used to estimate limb weakness quantitatively, and the corresponding exercise can be recommended. This targeted trajectory is extracted from a subject-specific scaled geometric Open-Sim musculoskeletal model and can be utilized for synthesizing customized robotic assistance. Two case studies are included to demonstrate how the algorithmic steps are implemented to map weakness to the task planning in the rehabilitation area.

Authors' contributions. Sakshi Gupta designed and carried out the research and drafted the initial version of the manuscript. Anupam Agrawal and Ekta Singla reviewed and edited the manuscript.

Financial support. None.

Ethical considerations. None.

Conflicts of interest. None.

https://doi.org/10.1017/S0263574722000844 Published online by Cambridge University Press

References

[1] D. Guiraud, "Interfacing the neural system to restore deficient functions: From theoretical studies to neuroprothesis design," *C. R. Biol.* **335**(1), 1–8 (2012).

[2] A.-S. Wahl and M. E. Schwab, "Finding an optimal rehabilitation paradigm after stroke: Enhancing fiber growth and training of the brain at the right moment," *Front. Hum. Neurosci.* **8**, 381 (2014).

[3] A. F. R. Olaya and A. L. Delis, "Emerging Technologies for Neuro-Rehabilitation after Stroke: Robotic Exoskeletons and Active Fes-Assisted Therapy," **In:** *Assistive Technologies for Physical and Cognitive Disabilities*, (IGI Global, 2015) pp. 1–21.

[4] A. C. Lo, P. D. Guarino, L. G. Richards, J. K. Haselkorn, G. F. Wittenberg, D. G. Federman, R. J. Ringer, T. H. Wagner, H. I. Krebs, B. T. Volpe, C. T. Bever Jr., D. M. Bravata, P. W. Duncan, B. H. Corn, A. D. Maffucci, S. E. Nadeau, S. S. Conroy, J. M. Powell, G. D. Huang and P. Peduzzi, "Robot-assisted therapy for long-term upper-limb impairment after stroke," *New Engl. J. Med.* **362**(19), 1772–1783 (2010).

[5] S. Jezernik, G. Colombo and M. Morari, "Automatic gait-pattern adaptation algorithms for rehabilitation with a 4-dof robotic orthosis," *IEEE Trans. Robot. Autom.* **20**(3), 574–582 (2004).

[6] C. Duret and S. Mazzoleni, "Upper limb robotics applied to neurorehabilitation: An overview of clinical practice," *NeuroRehabilitation* **41**(1), 5–15 (2017).

[7] J. M. Rieger, G. Constantinescu, M. J. Redmond, D. K. Scott, B. R. King, M. V. Fedorak and H. Lundgren, Systems and methods for diagnosis and treatment of swallowing disorders, July 6 2017. US Patent App. 15/313, 892.

[8] R. Song and K. Y. Tong, "EMG and kinematic analysis of sensorimotor control for patients after stroke using cyclic voluntary movement with visual feedback," *J. Neuroeng. Rehabil.* **10**(1), 1–10 (2013).

[9] D. J. Gladstone, C. J. Danells and S. E. Black, "The fugl-meyer assessment of motor recovery after stroke: A critical review of its measurement properties," *Neurorehab. Neural Repair* **16**(3), 232–240 (2002).

[10] M. V. Radomski and C. A. T. Latham. *Occupational Therapy for Physical Dysfunction* (Lippincott Williams & Wilkins, (2008).

[11] J. Kim, H. Kim and J. Kim, "Quantitative Assessment Test for Upper-Limb Motor Function By Using Emg and Kinematic Analysis in the Practice of Occupational Therapy," **In:** *2017 39th Annual International Conference of the IEEE Engineering in Medicine and Biology Society (EMBC)* (IEEE, 2017) pp. 1158–1161.

[12] A. Majidirad, Y. Yihun and L. Cure, "Toward an integrated intervention and assessment of robot-based rehabilitation," *J. Eng. Sci. Med. Diagn. Therapy* **3**(2), 1 (2020).

[13] F. Garcia-Sanjuan, J. Jaen and V. Nacher, "Tangibot: A tangible-mediated robot to support cognitive games for ageing people—A usability study," *Pervasive Mob. Comput.* **34**, 91–105 (2017).

[14] C. G. Canning, L. Ada and N. J. O'Dwyer, "Abnormal muscle activation characteristics associated with loss of dexterity after stroke," *J. Neurol. Sci.* **176**(1), 45–56 (2000).

[15] J. Chae, G. Yang, B. K. Park and I. Labatia, "Muscle weakness and cocontraction in upper limb hemiparesis: relationship to motor impairment and physical disability," *Neurorehab. Neural Repair* **16**(3), 241–248 (2002).

[16] C. Fleischer, "Controlling exoskeletons with EMG signals and a biomechanical body model", Ph.D. Dissertation (2007).

[17] E. E. Cavallaro, J. Rosen, J. C. Perry and S. Burns, "Real-time myoprocessors for a neural controlled powered exoskeleton arm," *IEEE Trans. Biomed. Eng.* **53**(11), 2387–2396 (2006).

[18] Y. M. Aung and A. Al-Jumaily, "Estimation of upper limb joint angle using surface emg signal," *Int. J. Adv. Robot Syst.* **10**(10), 369 (2013).

[19] I. Elamvazuthi, G. A. Ling, K. A. R. K. Nurhanim, P. Vasant and S. Parasuraman, "Surface Electromyography (semg) Feature Extraction Based on Daubechies Wavelets," **In:** *2013 IEEE 8th Conference on Industrial Electronics and Applications (ICIEA)*, (IEEE, 2013) pp. 1492–1495.

[20] K. Nurhanim, I. Elamvazuthi, P. Vasant, T. Ganesan, S. Parasuraman and M. K. A. Ahamed Khan, "Joint torque estimation model of Surface Electromyography (SEMG) based on swarm intelligence algorithm for robotic assistive device," *Procedia Comput. Sci.* **42**, 175–182 (2014).

[21] H. Kim, H. Park, S. Lee and D. Kim, "Joint torque estimation using semg and deep neural network," *J. Electr. Eng. Technol.* **15**(5), 2287–2298 (2020).

[22] W. Rose, Electromyogram analysis, University of Delaware., Online course material, Retrieved July, 5: 2016, 2011.

[23] S. B. N. Thompson and M. Morgan. *Occupational Therapy for Stroke Rehabilitation* (Springer, US, 2013).

[24] S. B. O'Sullivan, T. J. Schmitz and G. Fulk. *Physical Rehabilitation* (FA Davis, Philadelphia, 2019).

[25] P. De Leva, "Adjustments to zatsiorsky-seluyanov's segment inertia parameters," *J. Biomech.* **29**(9), 1223–1230 (1996).

[26] S. Plagenhoef, F. Gaynor Evans and T. Abdelnour, "Anatomical data for analyzing human motion," *Res. Q. Exercise Sport.* **54**(2), 169–178 (1983).

Cite this article: S. Gupta, A. Agrawal and E. Singla (2023). "Muscle weakness assessment tool for automated therapy selection in elbow rehabilitation", Robotica **41**, 833–849. https://doi.org/10.1017/S0263574722000844